

Brillouin Cooling in a Linear Waveguide

Yin-Chung Chen, Seunghwi Kim, Gaurav Bahl*

Mechanical Science and Engineering, University of Illinois at Urbana-Champaign,
Urbana, Illinois, USA

*To whom correspondence should be addressed; E-mail: bahl@illinois.edu

Abstract

Brillouin scattering is rarely considered as a mechanism that can cause cooling of a material due to the thermodynamic dominance of Stokes scattering in most practical systems. However, it has been shown in experiments on resonators that net phonon annihilation through anti-Stokes Brillouin scattering can be enabled by means of a suitable set of optical and acoustic states. The cooling of traveling phonons in a linear waveguide, on the other hand, could lead to the exciting future prospect of manipulating unidirectional heat fluxes and even the nonreciprocal transport of quantum information via phonons. In this work, we present the first analysis of the conditions under which Brillouin cooling may be achieved in a linear waveguide. We analyze the three-wave mixing interaction between the optical and acoustic modes that participate in forward Brillouin scattering, and reveal the key regimes of operation for the process. Our calculations indicate that measurable cooling may occur in state-of-the-art systems when pumped with a few tens of mW of optical power. However, if the Brillouin gain of these systems could be increased by only one order-of-magnitude, cooling can be achieved with very low powers in the single-mW range.

1 Introduction

Spontaneous Brillouin scattering of light from acoustic phonons [1, 2] results in creation of *photons* at both higher (anti-Stokes) and lower (Stokes) energies than the pump. As the scattering process is inelastic, additional *phonons* are simultaneously created in the material during Stokes transitions, while the existing phonons are annihilated in the anti-Stokes transitions. Such annihilation of phonons from a mode can be broadly termed as a

cooling phenomenon as it reduces the vibrational energy present in the solid [3–6]. In a bulk isotropic material, the probability of spontaneous Stokes scattering is always higher than that of anti-Stokes scattering [7]. Furthermore, the possibility of achieving Stokes-directed *stimulated* Brillouin Scattering (SBS) is quite high due to the very large gain of the process. As a result, net phonon creation and heating of the system are nearly always encountered in experiments. The solution to the fundamental challenge of achieving net phonon annihilation lies in modifying the Stokes vs. anti-Stokes scattering probabilities through the photonic density of states of the medium [8–10]. In practice, this can be achieved through a photonic-engineered structure like a resonator or photonic crystal [11–13]. Exploitation of this idea previously led to the demonstration of Brillouin cooling in whispering-gallery resonators [6], where selection of discrete modes in energy-momentum space permitted the complete suppression of Stokes scattering (Fig. 1a). Indeed, a second requirement revealed in studies of resonant Brillouin cooling [14, 15] is that the photon lifetime within the system must be smaller than the phonon lifetime. In other words, photons must radiate and transfer energy out of the system without being reabsorbed or scattering back. Finally, higher opto-acoustic coupling, i.e. higher Brillouin gain, also helps improve the cooling rates.

In this paper we address the question of whether Brillouin cooling can be achieved in a linear waveguide. This question is motivated by three reasons, which collectively point towards the possibility of cooling traveling phonons in such a system. First, recent experimental developments on linear waveguides have begun to report extremely large Brillouin gains [16–18], suggesting that sufficient gain may be available for practical cooling experiments. Second, optical fibers easily support photon coherence over over kilometer lengthscales, while phonon coherence cannot be supported over such lengths due to material dissipation, thus satisfying the lifetime criterion. Even on-chip optical waveguides have the potential to access this extremely low optical loss regime [19]. In contrast to resonators where the optical and acoustic field coherence is evaluated over time, in linear systems the coherence must be evaluated over a length parameter. Finally, it is practical to engineer the optical modes of a linear waveguide to achieve Stokes suppression and anti-Stokes enhancement, similar to how cooling was achieved in resonators. Fig. 1 shows that while linear waveguides do not support discrete modes as resonators do, it is possible to arrange for Stokes suppression using two optical modes that have different transverse order. Our analysis here presents the conditions under which appreciable cooling could potentially be achieved, and hopes to help direct further experimental

studies on linear waveguides.

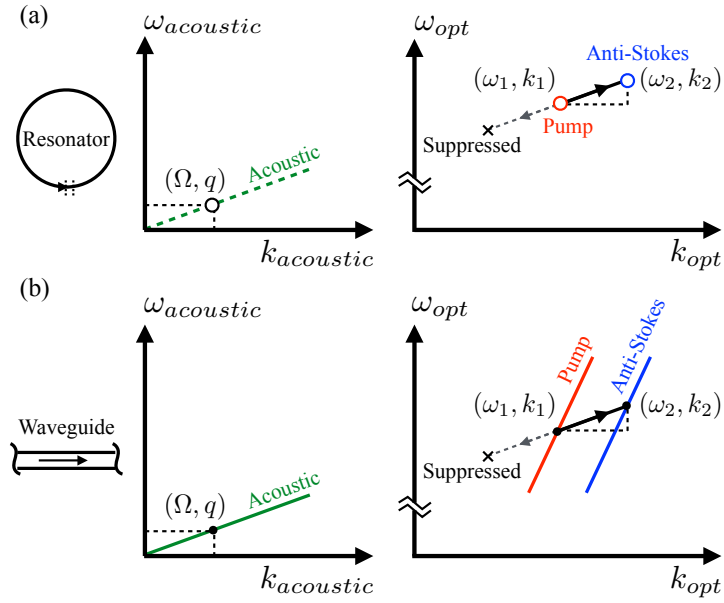


Figure 1: Phase-matching conditions for Brillouin cooling. **(a)** In a resonator, the available modes are represented by discrete points (circles) in the $\omega - k$ space. Stokes scattering can be suppressed by the naturally available high-order modes of a resonator, and only the anti-Stokes photons are permitted, leading to net phonon annihilation [6]. **(b)** In a waveguide, due to lack of modal confinement in the direction of propagation, the discrete mode points become discrete mode lines. By pumping a suitable optical mode family, the Stokes scattering process can be suppressed, potentially enabling cooling if other required conditions are met.

2 Coupled wave equations for anti-Stokes Brillouin scattering

We consider a three-wave mixing process between the pump wave, anti-Stokes wave, and the acoustic wave in a linear waveguide. It is assumed that no mode exists for light scattered in the Stokes direction, which suppresses Stokes scattering [6], as shown in Fig. 1b. As shown in Fig. 2, the three waves are assumed to co-propagate in a waveguide infinitely extended in the z -direction for the forward scattering case. We consider here only the

forward scattering case since the acoustic mode participating in backward scattering has greater frequency and thus lower Q-factor. As we will see later, cooling of such a lossy acoustic mode is impractical. Following similar treatment as in [14, 20] we let the optical fields and the acoustic field take the forms

$$\begin{aligned}
\mathbf{E}_1 &= \tilde{\mathbf{E}}_1(x, y) a_1(z, t) e^{i(k_1 z - \omega_1 t)} + \text{c.c.}, \\
\mathbf{E}_2 &= \tilde{\mathbf{E}}_2(x, y) a_2(z, t) e^{i(k_2 z - \omega_2 t)} + \text{c.c.}, \\
\mathbf{u} &= \tilde{\mathbf{u}}(x, y) b(z, t) e^{i(qz - \Omega t)} + \text{c.c.},
\end{aligned}
\tag{1}$$

where \mathbf{E}_1 , \mathbf{E}_2 , and \mathbf{u} are the pump, anti-Stokes, and acoustic fields, respec-

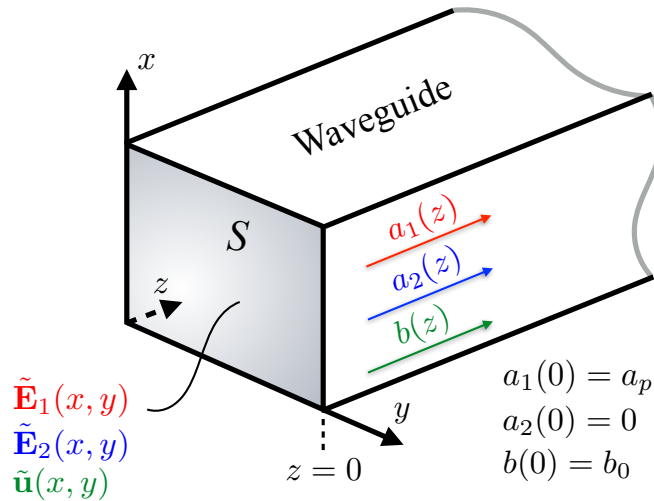


Figure 2: Three wave mixing interaction in a linear waveguide. The waveguide is assumed to be infinitely extended in the z -direction, with a cross section area S . The pump field \mathbf{E}_1 , anti-Stokes field \mathbf{E}_2 , and the acoustic field \mathbf{u} are separated into their transverse mode shapes $\tilde{\mathbf{E}}_1(x, y)$, $\tilde{\mathbf{E}}_2(x, y)$, and $\tilde{\mathbf{u}}(x, y)$, and the slowly varying amplitudes $a_1(z)$, $a_2(z)$, and $b(z)$, respectively. Under the constant pump assumption, the boundary condition at $z = 0$ is given by $a_1(0) = a_p = \text{constant}$, $a_2(0) = 0$, and $b(0) = b_0$, where a_p is the pump amplitude and b_0 is the acoustic amplitude at thermal equilibrium.

tively. The complex mode shape of the fields in the transverse directions are described by $\tilde{\mathbf{E}}_1$, $\tilde{\mathbf{E}}_2$, and $\tilde{\mathbf{u}}$, and are defined by the both geometry and material parameters of the waveguide. The dimensionless variables a_1 , a_2 , and b are the slowly varying amplitudes of the fields along the z -direction. For the anti-Stokes scattered light (ω_2, k_2) energy and momentum conservation

requirements set the relations $\omega_1 + \Omega = \omega_2$ and $k_1 + q = k_2$. The coupling equations for the slowly varying amplitudes can then be derived in the same manner as in [20].

$$\frac{\partial a_1}{\partial z} + \frac{1}{v_1} \frac{\partial a_1}{\partial t} = -i \frac{\omega_1 Q_1}{\mathcal{P}_1} a_2 b^* e^{i\delta k}, \quad (2a)$$

$$\frac{\partial a_2}{\partial z} + \frac{1}{v_2} \frac{\partial a_2}{\partial t} = -i \frac{\omega_2 Q_2}{\mathcal{P}_2} a_1 b e^{-i\delta k}, \quad (2b)$$

$$\frac{\partial b}{\partial z} + \frac{1}{v_A} \frac{\partial b}{\partial t} = -i \frac{\Omega Q_A}{\mathcal{P}_A} a_1^* a_2 e^{i\delta k}, \quad (2c)$$

where $v_1 = \omega_1/k_1$, $v_2 = \omega_2/k_2$, and $v_A = \Omega/q$ are the speeds of the waves and $\delta = k_2 - k_1 - q$ is the momentum mismatch between the hosting modes. Here, $\mathcal{P}_i = 2v_i \int_S \epsilon \tilde{\mathbf{E}}_i \cdot \tilde{\mathbf{E}}_i^* ds$ and $\mathcal{P}_A = 2v_A \rho_0 \Omega^2 \int_S \tilde{\mathbf{u}} \cdot \tilde{\mathbf{u}}^* ds$ are the integrals of the optical and acoustic Poynting vector [21, 22] over the cross section S of the waveguide, which are related to the power of the optical and acoustic modes, respectively. Q_1 , Q_2 , and Q_A are the coupling coefficients of the three waves, and can be expressed as integrals of the overlap of the three modes over the cross section S . These coefficients are related to each other by the relation $Q_1 = Q_2^* = Q_A$ [20]. As an example, if only the electrostrictive force is considered, and we assume vanishing fields at the boundary of the waveguide, the coupling coefficient Q_1 takes the form

$$Q_1 = \epsilon_0 \gamma_e \int_S (\nabla \cdot \tilde{\mathbf{u}}^*) \tilde{\mathbf{E}}_2 \cdot \tilde{\mathbf{E}}_1^* ds, \quad (3)$$

where γ_e is the electrostriction coefficient. Note that we have the freedom to normalize the transverse mode shape of the fields, and the actual total powers are given by $P_i = \mathcal{P}_i |a_i|^2$ and $P_A = \mathcal{P}_A |b|^2$.

To simplify the coupling terms in the above equations, we choose the normalization of the three fields such that $\omega_1/\mathcal{P}_1 \approx \omega_2/\mathcal{P}_2 \approx \Omega/\mathcal{P}_A$. Then the coefficients in front of the coupling terms can be written with a common coupling coefficient $\beta = \omega_1 Q_1^*/\mathcal{P}_1 = \omega_2 Q_2/\mathcal{P}_1 = \Omega Q_A^*/\mathcal{P}_A$. Substituting β into the Eqn. 2, and assuming steady-state condition ($\partial_t a_i, \partial_t b = 0$), we

obtain

$$\frac{\partial a_1}{\partial z} = -\gamma_1 a_1 - i\beta^* a_2 b^*, \quad (4a)$$

$$\frac{\partial a_2}{\partial z} = -\gamma_2 a_2 - i\beta a_1 b, \quad (4b)$$

$$\frac{\partial b}{\partial z} = -\Gamma b - i\beta^* a_1^* a_2 + \xi, \quad (4c)$$

where we have also introduced the losses per unit length, γ_1 , γ_2 , and Γ into the equations, and assumed perfect phase-matching between the three waves. The last term ξ in the acoustic field equation is the Langevin source term [14, 23] that describes the per unit length regeneration of the acoustic field. This noise source is usually treated as a random function with the correlation $\langle \xi^*(z, t) \xi(z', t') \rangle = A \delta(z - z') \delta(t - t')$, where the angle bracket denotes either time average or ensemble average for a stationary ergodic noise source [14, 24]. The strength of the noise A is proportional to the dissipation Γ and the absolute square of the amplitude in thermal equilibrium $|b_0|^2$, where b_0 is the acoustic amplitude at thermal equilibrium. Here, instead of describing the using these rapid random fluctuations, we use a coarse-grained constant noise source to describe the phonon regeneration. The strength of this source term can be understood by turning off the coupling ($\beta = 0$) to obtain $\partial_z b = -\Gamma b + \xi$. The acoustic amplitude b should then stay at the constant value at thermal equilibrium b_0 . Therefore, we have $\xi = \Gamma b_0$ for the strength of the noise. These coupling equations (Eqns. 4) describe the general behavior of the anti-Stokes Brillouin cooling process for the forward scattering configuration in a waveguide.

3 Closed-form solution with non-depleted pump

To examine how the fields behave in a linear waveguide, we first assume that no pump depletion takes place, i.e. change in a_1 is negligible over position. By letting $a_1(z) = a_p = \text{constant}$, we can then simplify Eqns. 4 to the following:

$$\frac{\partial a_2}{\partial z} = -\gamma_2 a_2 - i\beta a_p b, \quad (5a)$$

$$\frac{\partial b}{\partial z} = -\Gamma b - i\beta^* a_p^* a_2 + \xi. \quad (5b)$$

The above equations can now be solved with the boundary conditions, $a_2(0) = 0$, and $b(0) = b_0$. The physical interpretation of these conditions

is that no anti-Stokes light is initially present in the waveguide at location $z = 0$, and that the starting location phonon occupation is the same as the unperturbed thermalized waveguide. The closed-form solutions are:

$$b(z) = b_0 \left[\frac{p_1^2 + \Gamma\gamma_2 + \gamma_2 p_1 + \Gamma p_1}{p_1(p_1 - p_2)} \exp(p_1 z) - \frac{p_2^2 + \Gamma\gamma_2 + \gamma_2 p_2 + \Gamma p_2}{p_2(p_1 - p_2)} \exp(p_2 z) + \frac{\Gamma\gamma_2}{p_1 p_2} \right], \quad (6)$$

$$a_2(z) = -i\beta a_p b_0 \left[\frac{\gamma_2 p_1 p_2 + p_1^2 p_2 - 2\Gamma\gamma_2 p_1 - \Gamma\gamma_2 p_2 + \Gamma p_1 p_2}{p_1 p_2 (p_1 - p_2)(p_1 + \gamma_2)} \exp(p_1 z) - \frac{\gamma_2 p_1 p_2 + p_1 p_2^2 - 2\Gamma\gamma_2 p_2 - \Gamma\gamma_2 p_1 + \Gamma p_1 p_2}{p_1 p_2 (p_1 - p_2)(p_2 + \gamma_2)} \exp(p_2 z) - \frac{2\Gamma\gamma_2(p_1 + p_2)}{p_1 p_2 (p_1 + \gamma_2)(p_2 + \gamma_2)} \exp(-\gamma_2 z) + \frac{\Gamma}{p_1 p_2} \right], \quad (7)$$

where the important parameters are $p_1 = \frac{1}{2}[-(\gamma_2 + \Gamma) + \sqrt{\Delta}]$ and $p_2 = \frac{1}{2}[-(\gamma_2 + \Gamma) - \sqrt{\Delta}]$, where $\Delta = (\gamma_2 - \Gamma)^2 - 4|\beta|^2|a_p|^2$. Note that the real part of p_1 and p_2 is always negative. The behavior of the acoustic and anti-Stokes fields is thus characterized by the common parameter Δ .

The case $\Delta > 0$ is generally achieved for small values of coupling $|\beta||a_p|$. At the location where all spatial transients die down ($z \rightarrow \infty$), $b(z)$ approaches the final cooled state

$$b(\infty) = \frac{b_0 \Gamma \gamma_2}{p_1 p_2} = \frac{b_0 \Gamma \gamma_2}{\Gamma \gamma_2 + |\beta|^2 |a_p|^2}. \quad (8)$$

Since for $\Delta > 0$ the modulus of p_1 is always a smaller than that of p_2 , the second term in Eqn.6 decays faster than the first term. Thus, we can then define a characteristic length of cooling $L_c = -\frac{1}{p_1}$, which is the length at which the first term in Eqn. 6 drops to $1/e$ of its initial value. For the extreme case of high acoustic damping where $\Gamma \gg |\beta||a_p|$, we have $b(\infty) = b_0$ i.e. no cooling occurs. For small $|\beta||a_p|$, we can expand $L_c \approx \Gamma/(|\beta|^2|a_p|^2)$, where we have also assumed $\Gamma \gg \gamma_2$ as in a typical optical waveguide.

Some typical solutions for $\Delta > 0$ are shown in Fig. 3, with Δ represented in units of Γ^2 . From the definition of Δ , $\Delta \approx \Gamma^2$ corresponds to low coupling or high acoustic loss. We see that the acoustic amplitude drops to $\sim 90\% \times b_0$

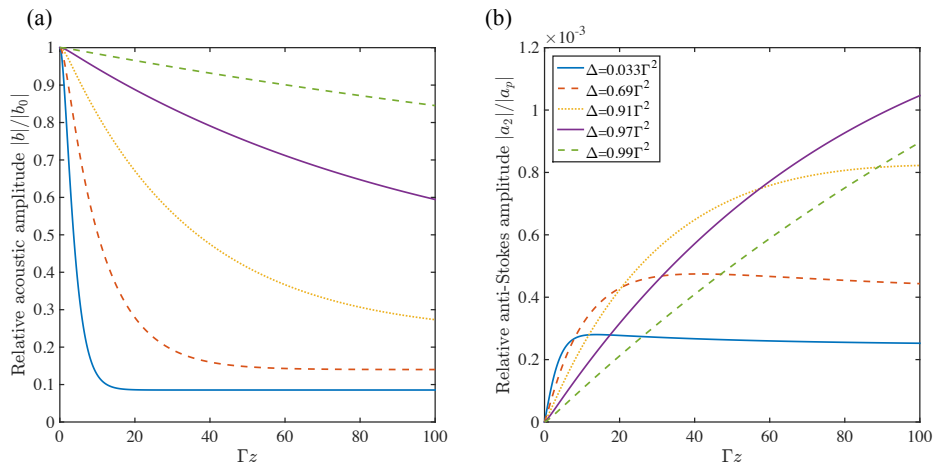


Figure 3: Solutions for the relative field amplitude of the acoustic field and the anti-Stokes for $\Delta > 0$ under the non-depleted pump assumption, where $\Delta = (\gamma_2 - \Gamma)^2 - 4|\beta|^2|a_p|^2$. **(a)** The acoustic field $|b|/|b_0|$, where b_0 is the amplitude at thermal equilibrium. The acoustic amplitude drops significantly for small positive Δ , which corresponds to a acoustic loss rate $\Gamma \sim |a_p||\beta|$. For large positive Δ , almost no cooling is observed. In the extreme case with $\Delta \approx \Gamma^2$, the acoustic amplitude only drops to 90 % of its original value after 100 decay lengths. **(b)** The anti-Stokes field $|a_2|/|a_p|$. In all the cases shown here, the anti-Stokes field starts to build up at the entrance region of the waveguide. However, for small Δ , as the acoustic field being cooled down, the amplitude of the anti-Stokes field also decreases. For $\Delta \approx \Gamma^2$, even though the phonon mode is not significantly cooled, the anti-Stokes amplitude increases almost linearly.

after 100 acoustic decay lengths $1/\Gamma$. Note that for these extremely low coupling cases the non-depleted pump assumption breaks down since the optical loss of the pump field is no longer negligible at $\Gamma z \approx 100$. This will be discussed further below. For higher coupling $\Delta \lesssim 0.7\Gamma^2$, the final cooled state amplitude can be reached at around 20 acoustic decay lengths.

Phenomenologically, the cooling of the acoustic mode occurs due to energy transfer from the acoustic field to the anti-Stokes field. Therefore, for higher coupling, the acoustic amplitude decreases faster while the anti-Stokes amplitude is also built up more rapidly. However, as the acoustic amplitude being cooled to its final state, there are fewer phonons to transfer energy to the anti-Stokes field. The anti-Stokes amplitude thus reaches a maximum value and subsequently decays according to the third term in Eqn. 7, which is simply the optical absorption. For lower coupling, even

though the growth of the anti-Stokes field is slower, there are more phonons available to transfer energy to the anti-Stokes field. Therefore, the maximum amplitude of the anti-Stokes field is larger for lower coupling, as shown in Fig. 3b.

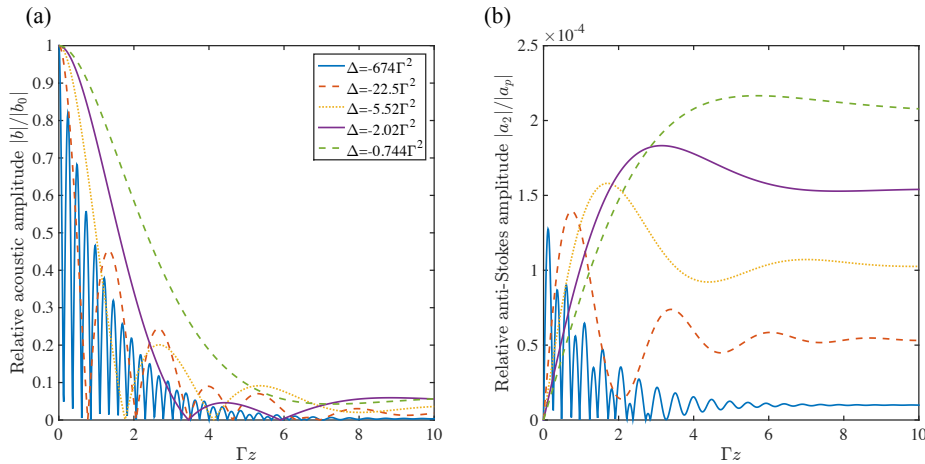


Figure 4: Solutions for the relative field amplitude of the acoustic field and the anti-Stokes for $\Delta < 0$ under the strong-pump assumption. **(a)** The acoustic field $|b|/|b_0|$, where b_0 is the amplitude at thermal equilibrium. **(b)** The anti-Stokes field $|a_2|/|a_p|$. For negative Δ , the solutions exhibit oscillatory behavior, corresponding to a rapid energy exchange between the acoustic field and the anti-Stokes field (with the anti-Stokes field roughly 90° out of phase, see Eqn. 7). In these cases, the acoustic amplitude is cooled down rapidly within 10 decay lengths. The anti-Stokes field reaches a steady value after the acoustic field vanishes.

For $\Delta < 0$, the solution exhibits oscillatory behavior since complex valued p_1 and p_2 are contained in the exponentials. The characteristic length of cooling is now given by $L_c = -2/(\gamma + \Gamma) \approx 2/\Gamma$, meaning that the acoustic field can approach its final cooled state within only a few decay lengths. The cooling in this regime is accompanied by a spatial field oscillation with characteristic length $\lambda_{osc} = 2/\sqrt{|\Delta|}$. For the case of extremely strong coupling $|\beta||a_p| \gg \Gamma$, the oscillation length is approximately $\lambda_{osc} \approx 1/(|\beta||a_p|)$, corresponding to a rapid oscillation occurring within the transient lengthscale L_c .

Fig. 4 shows solutions for a few cases of $\Delta < 0$. For all cases, the acoustic amplitude b drops to almost zero within a few acoustic decay lengths. In this regime there is rapid energy exchange between the acoustic field and the anti-Stokes field before they reach their final values. The behavior of the

anti-Stokes field is similar to the $\Delta > 0$ cases. The anti-Stokes amplitude grows faster for stronger coupling, but the maximum amplitude is smaller.

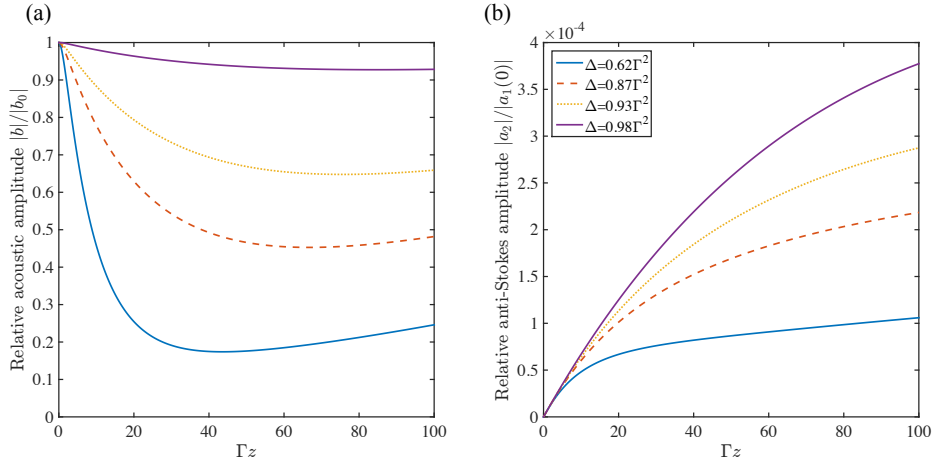


Figure 5: Numerical Solutions to Eqns. 4 showing the relative field amplitude of the acoustic and the anti-Stokes fields. The calculation is carried out using $\gamma_1 = 0.006\Gamma$, and Δ here is defined using the value of a_1 at $z = 0$, $\Delta = (\gamma_2 - \Gamma)^2 - 4|\beta|^2|a_1(0)|^2$. **(a)** The acoustic field $|b|/|b_0|$, where b_0 is the acoustic amplitude in thermal equilibrium. Unlike the constant pump cases (Fig. 3), the acoustic field increases after reaching its minimum due to the decrease in the pump amplitude. **(b)** The anti-Stokes field $|a_2|/|a_1(0)|$. The growth in the the anti-Stokes fields is slower than in the constant pump cases. In comparison with Fig. 3, the prediction of final cooled state for the acoustic field under the constant pump assumption is valid for $\Delta \lesssim 0.7\Gamma^2$.

Before concluding this section we examine in Fig. 5 a few numerical solutions for Eqns. 4, where pump depletion is incorporated. Indeed, the solutions, will depend on the optical loss of the pump field γ_1 . In Fig. 5 we fix the pump loss $\gamma_1 = 0.006\Gamma$, in accordance with the typical values seen in experiments [25, 26] (see next section). The value of Δ indicated in the figure is evaluated using the value of pump field a_1 at the entrance of the waveguide, $\Delta = (\gamma_2 - \Gamma)^2 - 4|\beta|^2|a_1(0)|^2$. As shown in Fig. 5b, instead of being cooled to a final state, the amplitude of the acoustic field increases after reaching a minimal value. This is due to the fact that the spatially decreasing pump amplitude decreases the cooling efficiency further down the waveguide. For the extremely weak coupling cases, our previous non-depleted pump assumption led to an overestimation of the minimum acoustic amplitude. Comparing Fig. 3 with Fig. 5, we see that for the typical

pump loss $\gamma_1 = 0.006\Gamma$ the non-depleted pump assumption is acceptable for $\Delta \lesssim 0.7\Gamma^2$.

As we will discuss in the next section, typical experiments almost always exhibit $\Delta \gg 0$, which corresponds to the weak coupling regime. To achieve greater cooling, lower acoustic loss Γ and higher coupling coefficient β are always more preferable.

4 Practical considerations for observing Brillouin cooling in linear waveguides

Now that we understand the general behavior of the solution, we can relate the calculation to available experimental data. We first note that if we suppress the noise source term ξ in Eqn. 4c, Eqns. 4 can be used to describe both Stokes process and anti-Stokes process for forward scattering. The field amplitude a_2 in either process describes the higher frequency optical field, i.e, in the Stokes process a_1 is the Stokes field and a_2 is the pump field, whereas in the anti-Stokes process a_1 is the pump field and a_2 is the anti-Stokes field. Presently, we consider the forward Stokes process only, since due to lower phonon dissipation the likelihood for observing cooling is greater. The relation between the coupling coefficient β and the SBS gain G ($\text{W}^{-1}\text{m}^{-1}$) has been given in [20]. Here, we reproduce the calculation for clarity. For the Stokes process under the non-depleted pump assumption ($a_2 = \text{constant}$), Eqns. 4 become

$$\frac{\partial a_1}{\partial z} = -i\beta^* a_2 b^*, \quad (9a)$$

$$\frac{\partial b}{\partial z} = -\Gamma b - i\beta^* a_1^* a_2, \quad (9b)$$

where we have neglected the the optical loss here. Here, a_2 is the pump field and a_1 is the Stokes field. If we assume that the Stokes field does not vary much within the acoustic decay length $1/\Gamma$, i.e. the length scale of the variation of the optical fields is greater than the acoustic length scale ($\partial_z a_1 \ll \Gamma$), then Eqn. 9b can be solved directly to obtain

$$b(z) \approx -i \frac{\beta^* a_1(z)^* a_2(z)}{\Gamma}, \quad (10)$$

and

$$\frac{\partial a_1}{\partial z} = \frac{|\beta|^2 |a_2|^2 a_1}{\Gamma}. \quad (11)$$

Now recall that the total optical power is given by $P_i = \mathcal{P}_i |a_i|^2$, we obtain

$$\frac{\partial P_1}{\partial z} = \frac{2\mathcal{P}_1 |\beta|^2 |a_1|^2 |a_2|^2}{\Gamma} = \frac{2|\beta|^2 P_1 P_2}{\mathcal{P}_2 \Gamma} = G P_1 P_2, \quad (12)$$

where $G = 2|\beta|^2/\mathcal{P}_2\Gamma = 2|\beta|^2/\mathcal{P}_1\Gamma$, and we have used $\mathcal{P}_1 \approx \mathcal{P}_2$. Eqn. 12 are simply the gain relations for the SBS process in the waveguide and G ($\text{W}^{-1}\text{m}^{-1}$) is the SBS gain measured in experiments. It is worth noting from (Eqn. 3) that the coupling coefficient β is given by the integral of the modes over the cross section of the waveguide, and is therefore independent of the loss Γ . The SBS gain, on the other hand, depends on the length over which the three modes are coupled, which is related to the acoustic decay length $1/\Gamma$. For a given SBS experiment setup, we can now extract the value of the coupling coefficient from the experimental measurements of G and Γ to obtain $\beta \approx \sqrt{\Gamma G \mathcal{P}_1}/2$.

Now suppose that the given SBS experiment setup is reversed, i.e. a_1 becomes the pump field and a_2 becomes the anti-Stokes field. Since the coupling coefficient is preserved, we can connect the experimental SBS measurements to the anti-Stokes process. In terms of pump power $P_1 = \mathcal{P}_1 |a_p|^2$ and SBS gain $G = 2|\beta|^2/\mathcal{P}_1\Gamma$ in the reversed experiment, the discriminant Δ becomes

$$\Delta = (\gamma_2 - \Gamma)^2 - 4|\beta|^2 |a_p|^2 = (\gamma_2 - \Gamma)^2 - 2G P_1 \Gamma. \quad (13)$$

We can now use the available experimental data to evaluate Δ and evaluate how much cooling could potentially be achieved. In the following discussion we fix the pump wavelength at 1550 nm, and focus only on silicon photonic waveguides.

The typical value of the optical attenuation in a high-Q waveguide is about 0.3 dB/cm [26], corresponding to a γ_2 of 0.035 cm^{-1} at 1550 nm. The acoustic loss can be obtained from the Q-factor of the acoustic modes $\Gamma = 2\pi\Omega/2v_A Q$. The factor of two in the denominator accounts for the fact that we are dealing with field amplitudes instead of intensities in our coupled wave equations (Eqns 4). Using $Q \approx 1000$ from the typical SBS experiment in a waveguide for a 10 GHz mode [25], we estimate $\Gamma \approx 5.92 \text{ cm}^{-1}$. Note that with these values the acoustic loss is much greater than the optical loss, which is consistent with our assumption $\Gamma \gg \gamma_2$ in the previous section. These values of losses were also used in calculating the numerical solution in the previous section. The SBS gain G in typical SBS experiment is around 3000 ($\text{W}^{-1}\text{m}^{-1}$) [18, 25]. Assuming a pump power of 1 mW, these

	SBS gain G ($\text{W}^{-1}\text{m}^{-1}$)	Acoustic loss Γ (cm^{-1})	Required power P_1 (mW)	Characteristic length L_c (cm)
Experiment [25]	2200	5.92	60	1.26
Experiment [18]	3600	19.8	36	1.39
Theory [17]	10000	5.92	13.1	1.26
Theory [17]	10^5	5.92	1.3	1.26

Table 1: Power required to reach the final cooled state $b(\infty)/b_0 = 0.05$. Here the optical loss is fixed at 0.035 cm^{-1} , and the frequency of the acoustic mode is fixed at 10 GHz. In the calculations for the last two rows, we use the gain value given in [17], and assume the acoustic loss is fixed at $5.92 \text{ (cm}^{-1}\text{)}$, corresponding to an acoustic mode of $Q = 1000$.

values give $\Delta \approx 0.98\Gamma^2$, which corresponds to the weak coupling cases in Fig. 3. As we discussed in the previous section, in this regime the non-depleted pump assumption is not valid, and cooling in this configuration is not very practical. However, if we increase the pump power to 30 mW, we obtain $\Delta \approx 0.68\Gamma^2$. In this regime, the non-depleted pump assumption is valid, and the final cooled state is given by Eqn. 8. In terms of gain G and pump power P_1 , the amplitude of the final cooled state can be written as

$$\frac{b(\infty)}{b_0} = \frac{\gamma_2}{\gamma_2 + GP_1/2}. \quad (14)$$

The characteristic length of reaching this state is given by $L_c = 2/(\gamma_2 + \Gamma - \sqrt{\Delta})$.

In table 1 we summarize some recent experimental parameters for SBS in waveguides and estimate the required power to reach 5% final relative acoustic amplitude $b(\infty)/b_0 = 0.05$. Here we fix the value of the optical loss at 0.035 cm^{-1} and the frequency of the acoustic mode at 10 GHz. For typical SBS gain in recent experiments, the power required for this level of cooling is 30-60 mW, and the characteristic length of cooling L_c is of the order of 1 cm. Note that for acoustic modes with higher loss, the characteristic length is longer as it is more challenging to cool them [15]. However if SBS gain of 10^4 - 10^5 is made available, as predicted in [17], then the required cooling power could be just a few mW.

5 Conclusions

We have investigated the anti-Stokes Brillouin scattering three-wave mixing process in linear waveguides for the possibility of achieving phonon annihilation and cooling. We show that the solutions can be separated into two regimes, essentially marked by weak coupling ($\Delta > 0$) and strong coupling ($\Delta < 0$). The coupling coefficients extracted from state-of-the-art SBS experiments lie in the low coupling regime. In this regime, no appreciable cooling would be observed with a pump power of 1 mW, and the depletion of the pump field due to optical absorption significantly reduces any potential cooling of the acoustic field. However, cooling efficiency could be increased significantly by increasing the pump power to the order of a few tens of mW. Alternatively, if SBS gain of $10^5 \text{ m}^{-1}\text{W}^{-1}$ or larger is available, which is only an order-of-magnitude higher than the best known results, then cooling could be achieved with pump power around 1 mW.

Our analysis suggests that, for potential cooling experiments, the design of waveguides should be focused on improving the quality factor of the acoustic mode, since cooling is made easier with lower loss phonon modes. Additionally, enhancement of SBS gain is also favorable for cooling as this corresponds to a higher coupling coefficient. The optical modes, on the other hand, should be designed such that only two mode families are available inside the waveguide. By pumping the faster optical branch, one can potentially reject the Stokes process and allow only anti-Stokes light to propagate along the waveguide.

A key difference between cavity optomechanical cooling and Brillouin cooling is that the latter annihilates traveling phonons, which are also responsible for heat transport in micro- and nano-scale devices. The possibility of accessing Brillouin cooling in linear systems thus opens up a new approach to laser cooling, and may have a significant impact on heat management in photonic circuits and on quantum information transport through phonons.

References

- [1] Y. R. Shen and N. Bloembergen, “Theory of stimulated Brillouin and Raman scattering,” *Physical Review*, vol. 137, no. 6A, p. A1787, 1965.
- [2] R. W. Boyd, *Nonlinear optics*. Academic press, 2003.
- [3] O. Arcizet, P.-F. Cohadon, T. Briant, M. Pinarid, and A. Heidmann,

- “Radiation-pressure cooling and optomechanical instability of a micromirror,” *Nature*, vol. 444, no. 7115, pp. 71–74, 2006.
- [4] S. Gigan, H. Böhm, M. Paternostro, F. Blaser, G. Langer, J. Hertzberg, K. Schwab, D. Bäuerle, M. Aspelmeyer, and A. Zeilinger, “Self-cooling of a micromirror by radiation pressure,” *Nature*, vol. 444, no. 7115, pp. 67–70, 2006.
- [5] D. Kleckner and D. Bouwmeester, “Sub-kelvin optical cooling of a micromechanical resonator,” *Nature*, vol. 444, no. 7115, pp. 75–78, 2006.
- [6] G. Bahl, M. Tomes, F. Marquardt, and T. Carmon, “Observation of spontaneous brillouin cooling,” *Nature Physics*, vol. 8, no. 3, pp. 203–207, 2012.
- [7] Y. Peter and M. Cardona, *Fundamentals of semiconductors: physics and materials properties*. Springer, 2010.
- [8] E. M. Purcell, “Spontaneous emission probabilities at radio frequencies,” *Physical Review*, vol. 69, p. 681, 1946.
- [9] S. Gaponenko, “Effects of photon density of states on raman scattering in mesoscopic structures,” *Physical Review B*, vol. 65, no. 14, p. 140303, 2002.
- [10] Y.-C. Chen and G. Bahl, “Raman cooling of solids through photonic density of states engineering,” *Optica*, vol. 2, no. 10, pp. 893–899, 2015.
- [11] Y. Gong, M. Makarova, S. Yerci, R. Li, M. J. Stevens, B. Baek, S. W. Nam, R. H. Hadfield, S. N. Dorenbos, V. Zwiller, *et al.*, “Linewidth narrowing and purcell enhancement in photonic crystal cavities on an er-doped silicon nitride platform,” *Optics express*, vol. 18, no. 3, pp. 2601–2612, 2010.
- [12] X. Checoury, M. El Kurdi, Z. Han, and P. Boucaud, “Enhanced spontaneous Raman scattering in silicon photonic crystal waveguides on insulator,” *Optics Express*, vol. 17, no. 5, pp. 3500–3507, 2009.
- [13] M. Boroditsky, R. Vrijen, T. F. Krauss, R. Coccioli, R. Bhat, and E. Yablonovitch, “Spontaneous emission extraction and purcell enhancement from thin-film 2-d photonic crystals,” *Lightwave Technology, Journal of*, vol. 17, no. 11, pp. 2096–2112, 1999.

- [14] G. Agarwal and S. S. Jha, “Multimode phonon cooling via three-wave parametric interactions with optical fields,” *Physical Review A*, vol. 88, no. 1, p. 013815, 2013.
- [15] M. Tomes, F. Marquardt, G. Bahl, and T. Carmon, “Quantum-mechanical theory of optomechanical brillouin cooling,” *Physical Review A*, vol. 84, no. 6, p. 063806, 2011.
- [16] P. T. Rakich, P. Davids, and Z. Wang, “Tailoring optical forces in waveguides through radiation pressure and electrostrictive forces,” *Optics express*, vol. 18, no. 14, pp. 14439–14453, 2010.
- [17] P. T. Rakich, C. Reinke, R. Camacho, P. Davids, and Z. Wang, “Giant enhancement of stimulated brillouin scattering in the subwavelength limit,” *Physical Review X*, vol. 2, no. 1, p. 011008, 2012.
- [18] R. Van Laer, B. Kuyken, D. Van Thourhout, and R. Baets, “Interaction between light and highly confined hypersound in a silicon photonic nanowire,” *Nature Photonics*, vol. 9, no. 3, pp. 199–203, 2015.
- [19] H. Lee, T. Chen, J. Li, O. Painter, and K. J. Vahala, “Ultra-low-loss optical delay line on a silicon chip,” *Nature communications*, vol. 3, p. 867, 2012.
- [20] C. Wolff, M. J. Steel, B. J. Eggleton, and C. G. Poulton, “Stimulated brillouin scattering in integrated photonic waveguides: Forces, scattering mechanisms, and coupled-mode analysis,” *Phys. Rev. A*, vol. 92, p. 013836, Jul 2015.
- [21] J. D. Jackson, *Classical electrodynamics*, ch. 8. New York, NY: Wiley, 3 ed., 1999.
- [22] B. A. Auld, *Acoustic fields and waves in solids*, vol. 2. RE Krieger, 1990.
- [23] R. W. Boyd, K. Rzaewski, and P. Narum, “Noise initiation of stimulated brillouin scattering,” *Physical Review A*, vol. 42, no. 9, p. 5514, 1990.
- [24] L. Mandel and E. Wolf, *Optical coherence and quantum optics*. Cambridge university press, 1995.
- [25] H. Shin, W. Qiu, R. Jarecki, J. A. Cox, R. H. Olsson III, A. Starbuck, Z. Wang, and P. T. Rakich, “Tailorable stimulated brillouin scattering in nanoscale silicon waveguides,” *Nature communications*, vol. 4, 2013.

- [26] Y. Vlasov and S. McNab, “Losses in single-mode silicon-on-insulator strip waveguides and bends,” *Optics express*, vol. 12, no. 8, pp. 1622–1631, 2004.